Sintering and Formation of a Nonporous Carbonate Shell at the Surface of CaO-Based Sorbent Particles during CO2-Capture Cycles

ARTICLE *in* ENERGY & FUELS · SEPTEMBER 2010

Impact Factor: 2.79 · DOI: 10.1021/ef100931v

2 AUTHORS:

Vasilije Manovic
Cranfield University
91 PUBLICATIONS **1,974** CITATIONS
SEE PROFILE

Edward Anthony
Cranfield University
260 PUBLICATIONS **7,172** CITATIONS
SEE PROFILE

Energy Fuels **2010,** *24,* 5790–5796 · DOI:10.1021/ef100931v
Published on Web 09/24/2010

energy&fuels
article

Sintering and Formation of a Nonporous Carbonate Shell at the Surface of CaO-Based Sorbent Particles during CO_2-Capture Cycles

Vasilije Manovic and Edward J. Anthony*

CanmetENERGY, Natural Resources Canada, 1 Haanel Drive, Ottawa, Ontario K1A 1M1, Canada

Received July 22, 2010. Revised Manuscript Received August 23, 2010

The existence and formation of a carbonate shell at the surface of the particles of CaO-based sorbents is investigated in this paper. Two sorbents were tested: natural Kelly Rock (KR) limestone and synthetic pellets (KR-CA-14) prepared from the same limestone and calcium aluminate cement (CA-14). Various different series of calcination/carbonation cycles were carried out in a thermogravimetric analyzer (TGA) apparatus, and the sorbent samples produced after those cycles were analyzed with a scanning electron microscope (SEM). It is shown that sintering during cycles is more pronounced at the surface of sorbent particles, which results in the formation of nonporous areas or even a totally nonporous shell that surrounds a partially reacted CaO core. However, the dependency of shell formation upon cycle number is difficult to elucidate by SEM because increasing cycle numbers achieve lower conversion levels, which reduce the chance of shell formation. Prolonged carbonation after a series of cycles showed that there is a limit in maximum conversion levels, which cannot be solely explained by product layer formation at the interior sorbent surface area. The SEM images of samples after prolonged carbonation periods clearly show the presence of more sintered areas at the outer particle surface and/or carbonate shell/partially reacted particle pattern. This is explained by the phenomenon of more pronounced sintering at the sorbent particle surface than seen in the particle interior because of surface tension and more pronounced loss of pore volume near the exterior of the particle. The formation of a carbonate shell at the particle surface is a different phenomenon from that of the formation of a product layer at the pore surface area and also limits diffusion during carbonation.

Introduction

It is widely accepted that climate change is being driven by increasing concentrations of greenhouse gases because of human activity, and this key problem requires urgent solutions. Carbon dioxide (CO_2) is the main greenhouse gas that causes global warming, and fossil-fuel-fired power plants represent a major source of anthropogenic CO_2. The negative environmental effects of such emissions represent a growing problem because the use of fossil fuels, such as coal, is increasing and can be expected to do so for the near- to medium-term future.[1,2] Therefore, technologies associated with CO_2 capture and storage (CCS) are increasingly considered to be likely contributors to reduce these emissions.[3,4]

Although, in principle, the entire gas stream containing low concentrations of CO_2 could be transported and sequestered underground, the energy and other associated costs generally make this approach impractical. Therefore, CO_2 has to be concentrated to be suitable for compression and piping to a storage site,[5] which is the goal of CO_2 capture. There are three main approaches to obtain concentrated CO_2 streams from fossil fuels: (i) postcombustion CO_2 capture from the flue gas, (ii) precombustion separation, which involves gasification and capture of CO_2 before the combustion of the produced gases, and (iii) oxy-fuel combustion, which uses oxygen instead of air during combustion.[6,7]

Currently, "scrubbing" of flue gases using amine-based sorbents, such as monoethanolamine (MEA), is the postcombustion technology closest to the market. This technology has been widely used in the natural gas industry for over 60 years, and it is being considered for separation of CO_2 from flue gas. However, this approach is very energy-intensive and has other problems that appear to be likely to result in significantly higher electricity costs (by 70%).[8] That has led to the investigation of other methods of CO_2 capture, such as the reversible reaction between calcium oxide and carbon dioxide to form calcium carbonate (the calcium-looping cycle).[6,9,10]

*To whom correspondence should be addressed. Telephone: (613) 996-2868. Fax: (613) 992-9335. E-mail: banthony@nrcan.gc.ca.

(1) Mohr, S. H.; Evans, G. M. Forecasting coal production until 2100. *Fuel* **2009**, *88*, 2059–2067.
(2) Hook, M.; Aleklett, K. Historical trends in American coal production and a possible future outlook. *Int. J. Coal Geol.* **2009**, *78*, 201–216.
(3) Intergovernmental Panel on Climate Change (IPCC). *Special Report on Carbon Dioxide Capture and Storage*; Metz, B., Davidson, O., de Coninck, H., Loos, M., Meyer, L., Eds.; Cambridge University Press: Cambridge, U.K., 2005.
(4) Herzog, H. What future for carbon capture and sequestration? *Environ. Sci. Technol.* **2001**, *35*, 148–153.
(5) Bachu, S. CO_2 storage in geological media: Role, means, status, and barriers to deployment. *Prog. Energy Combust. Sci.* **2008**, *34*, 254–273.
(6) Anthony, E. J. Solid looping cycles: A new technology for coal conversion. *Ind. Eng. Chem. Res.* **2008**, *47*, 1747–1754.
(7) Yang, H.; Xu, Z.; Fan, M.; Gupta, R.; Slimane, R.; Bland, B.; Alan, E.; Wright, I. Progress in carbon dioxide separation and capture: A review. *J. Environ. Sci.* **2008**, *20*, 14–27.
(8) Alie, C.; Backham, L.; Croiset, E.; Douglas, P. L. Simulation of CO_2 capture using MEA scrubbing: A flowsheet decomposition method. *Energy Convers. Manage.* **2005**, *46*, 475–487.
(9) Stanmore, B. R.; Gilot, P. Review - Calcination and carbonation of limestone during thermal cycling for CO_2 sequestration. *Fuel Process. Technol.* **2005**, *86*, 1707–1743.
(10) Blamey, J.; Anthony, E. J.; Wang, J.; Fennell, P. S. The use of the calcium looping cycle for post-combustion CO_2 capture. *Prog. Energy Combust. Sci.* **2010**, *36*, 260–279.

Preliminary economic analyses[11−13] suggest that such processes are economically attractive and can achieve CO_2 capture at relatively low cost, ~$20/ton avoided CO_2. An important advantage of using CaO-based sorbents is that limestone ($CaCO_3$) is both abundant and relatively inexpensive, and it is an environmentally benign natural material, suggesting that its use will be associated with much lower health and environmental risks in comparison to, for example, the use of synthetic amine-based sorbents.[14]

The calcium-looping cycle technology is based on the reversible chemical reaction.

$$CaO + CO_2 = CaCO_3 \quad (1)$$

Shimizu et al.[15] proposed a dual fluidized-bed reactor for CO_2 separation from flue gas in a multi-cycle process. This involves the reaction of CaO with CO_2 from flue gas in a carbonator and regeneration of sorbent in a calciner.[16] Carbonation (eq 1) is a relatively simple reaction process, which, in the ideal case, is limited only by the chemical equilibrium and kinetics determined by the temperature and CO_2 partial pressure. However, this reaction in practice is subject to some difficulties, including sensitivity (loss of reactivity) because of sulfation[17−19] and attrition and consequent elutriation from the fluidized-bed combustion (FBC) reactor.[20]

However, the most well-investigated problem is the loss of activity of the sorbent with increasing numbers of reaction cycles.[21−23] This is typically explained by sorbent sintering and the loss of the sorbent surface area and a significant reduction of the relatively small pore volume necessary for storage of the bulky $CaCO_3$ product. These deactivation mechanisms imply that carbonation through the sorbent particle volume is uniform; i.e., there is no conversion profile along the particle radius. Moreover, Abanades and Alvarez[21,24] demonstrated that maximum conversion reached after the fast, kinetically controlled reaction stage depends upon the maximum product layer thickness (at the pore surface area). To reduce sintering during cycles or reactivate sintered sorbent, different techniques have been investigated.[25] The most promising ones appear to include thermal pretreatment,[26,27] hydration,[28,29] and possibly preparing synthetic sorbents by means of doping CaO with compounds that prevent sintering. The most investigated are synthetic sorbents doped with Al_2O_3,[30−32] but recently, it has been shown that sorbents containing $KMnO_4$[33] and TiO_2[34] are also more resistant to sintering.

The intensity of sintering and the loss of CO_2 carrying capacity depends upon factors such as the temperature and CO_2 concentration during the calcination steps.[35] It has also been shown that synthetic sorbents are less resistant to severe conditions[36] and that they need reactivation steps to maintain high activity.[37] Moreover, this last study highlighted the fact that, during higher conversion, especially when severe calcination conditions are applied, enhanced sintering at the sorbent particle surface can additionally limit conversion. This limit and the formation of a carbonate shell around the sorbent particles are investigated in this study. It should be noted here that deactivation by the carbonate shell investigated here is related to the sorbent particle surface, and it is an additional limit during the carbonation process, which differs from limitations because of the formation of the product layer at the sorbent particle surface area.

Experimental Section

Kelly Rock (KR) limestone, with a particle size of 600−750 μm, was used without treatment and as a modified sorbent in the form of aluminate-supported pellets. The results of X-ray fluorescence (XRF) elemental analysis for this limestone are shown in

(11) MacKenzie, A.; Granatstein, D. L.; Anthony, E. J.; Abanades, J. C. Economics of CO_2 capture using the calcium cycle with a pressurized fluidized bed combustor. *Energy Fuels* **2007**, *21*, 920–926.
(12) Abanades, J. C.; Grasa, G.; Alonso, M.; Rodriguez, N.; Anthony, E. J.; Romeo, L. M. Cost structure of a postcombustion CO_2 capture system using CaO. *Environ. Sci. Technol.* **2007**, *41*, 5523–5527.
(13) Lisbona, P.; Martinez, A.; Lara, Y.; Romeo, L. M. Integration of carbonate CO_2 capture cycle and coal-fired power plants. A comparative study for different sorbents. *Energy Fuels* **2009**, *24*, 728–736.
(14) Veltman, K.; Singh, B.; Hertwich, E. G. Human and environmental impact assessment of postcombustion CO_2 capture focusing on emissions from amine-based scrubbing solvents to air. *Environ. Sci. Technol.* **2010**, *44*, 1496–1502.
(15) Shimizu, T.; Hirama, T.; Hosoda, H.; Kitano, K.; Inagaki, M.; Tejima, K. A Twin fluid-bed reactor for removal of CO_2 from combustion processes. *Chem. Eng. Res. Des.* **1999**, *77*, 62–68.
(16) Abanades, J. C.; Anthony, E. J.; Wang, J.; Oakey, A. Fluidized bed combustion systems integrating CO_2 capture with CaO. *Environ. Sci. Technol.* **2005**, *39*, 2861–2866.
(17) Grasa, G. S.; Alonso, M.; Abanades, J. C. Sulfation of CaO particles in a carbonation/calcination loop to capture CO_2. *Ind. Eng. Chem. Res.* **2008**, *47*, 1630–1635.
(18) Manovic, V.; Anthony, E. J. Sequential SO_2/CO_2 capture enhanced by steam reactivation of a CaO-based sorbent. *Fuel* **2008**, *87*, 1564–1573.
(19) Manovic, V.; Anthony, E. J. Competition of sulphation and carbonation reactions during looping cycles for CO_2 capture by CaO-based sorbents. *J. Phys. Chem. A* **2010**, *114*, 3997–4002.
(20) Lu, D. Y.; Hughes, R. W.; Anthony, E. J. Ca-based sorbent looping combustion for CO_2 capture in pilot-scale dual fluidized beds. *Fuel Process. Technol.* **2008**, *89*, 1386–1395.
(21) Abanades, J. C.; Alvarez, D. Conversion limits in the reaction of CO_2 with lime. *Energy Fuels* **2003**, *17*, 308–315.
(22) Fennell, P. S.; Pacciani, R.; Dennis, J. S.; Davidson, J. F.; Hayhurst, A. N. The effects of repeated cycles of calcination and carbonation on a variety of different limestones, as measured in a hot fluidized bed of sand. *Energy Fuels* **2007**, *21*, 2072–2081.
(23) Sun, P.; Grace, J. R.; Lim, C. J.; Anthony, E. J. The effect of CaO sintering on cyclic CO_2 capture in energy systems. *AIChE J.* **2007**, *53*, 2432–2442.
(24) Alvarez, D.; Abanades, J. C. Determination of the critical product layer thickness in the reaction of CaO with CO_2. *Ind. Eng. Chem. Res.* **2005**, *44*, 5608–5615.
(25) Manovic, V.; Anthony, E. J. Improvement of CaO-based sorbent performances for CO_2 looping cycles. *Therm. Sci.* **2009**, *13*, 89–104.
(26) Lysikov, A. I.; Salanov, A. N.; Okunev, A. G. Change of CO_2 carrying capacity of CaO in isothermal recarbonation−decomposition cycles. *Ind. Eng. Chem. Res.* **2007**, *46*, 4633–4638.
(27) Manovic, V.; Anthony, E. J. Thermal activation of CaO-based sorbent and self-reactivation during CO_2 capture looping cycles. *Environ. Sci. Technol.* **2008**, *42*, 4170–4174.
(28) Manovic, V.; Anthony, E. J. Steam reactivation of spent CaO-based sorbent for multiple CO_2 capture cycles. *Environ. Sci. Technol.* **2007**, *41*, 1420–1425.
(29) Fennell, P. S.; Davidson, J. F.; Dennis, J. S.; Hayhurst, A. N. Regeneration of sintered limestone sorbents for the sequestration of CO_2 from combustion and other systems. *J. Energy Inst.* **2007**, *80*, 116–119.
(30) Li, Z. S.; Cai, N. S.; Huang, Y. Y.; Han, H. J. Synthesis, experimental studies, and analysis of a new calcium-based carbon dioxide absorbent. *Energy Fuels* **2005**, *19*, 1447–1452.
(31) Dennis, J. S.; Pacciani, R. The rate and extent of uptake of CO_2 by a synthetic, CaO-containing sorbent. *Chem. Eng. Sci.* **2009**, *64*, 2147–2157.
(32) Manovic, V.; Anthony, E. J. CaO-based pellets supported by calcium aluminate cements for high-temperature CO_2 capture. *Environ. Sci. Technol.* **2009**, *43*, 7117–7122.
(33) Li, Y.; Zhao, C.; Chen, H.; Duan, L.; Chen, X. Cyclic CO_2 capture behavior of $KMnO_4$-doped CaO-based sorbent. *Fuel* **2010**, *89*, 642–649.
(34) Wu, S. F.; Zhu, Y. Q. Behavior of $CaTiO_3$/nano-CaO as a CO_2 reactive adsorbent. *Ind. Eng. Chem. Res.* **2010**, *49*, 2701–2706.
(35) Manovic, V.; Charland, J.-P.; Blamey, J.; Fennell, P. S.; Lu, D.; Anthony, E. J. Influence of calcination conditions on carrying capacity of CaO-based sorbent in CO_2 looping cycles. *Fuel* **2009**, *10*, 1893–1900.
(36) Manovic, V.; Anthony, E. J. CO_2 carrying behavior of calcium aluminate pellets under high-temperature high-CO_2 concentration calcination conditions. *Ind. Eng. Chem. Res.* **2010**, *49*, 6916–6922.
(37) Manovic, V.; Anthony, E. J. Reactivation and remaking of calcium aluminate pellets for CO_2 capture. *Fuel* **2010**, in press.

Table 1. XRF Elemental Analysis of the Kelly Rock Limestone Sample Used

component	content
SiO_2 (wt %)	2.95
Al_2O_3 (wt %)	0.74
Fe_2O_3 (wt %)	0.32
TiO_2 (wt %)	0.05
P_2O_5 (wt %)	<0.01
CaO (wt %)	52.43
MgO (wt %)	0.47
SO_3 (wt %)	0.30
Na_2O (wt %)	<0.096
K_2O (wt %)	0.21
Ba (ppm)	347
Sr (ppm)	286
V (ppm)	<0.50
Ni (ppm)	<0.50
Mn (ppm)	1023
Cr (ppm)	<0.50
Cu (ppm)	42
Zn (ppm)	30
loss on fusion (wt %)	42.05
sum (wt %)	99.69

Table 1. Commercial calcium aluminate cement, CA-14 (71% Al_2O_3 and 28% CaO), produced by Almatis, Inc., was used as a binder for pelletization. It was supplied as a very fine powder with >80% of the particles <45 μm. The prepared corresponding pellets were designated as KR-CA-14.

To prepare pellets, limestone was calcined at 850 °C for 2 h before hydration. Lime (after calcination) and cement were mixed in a glass beaker. The limestone/cement ratio was 9:1 (wt). Water was slowly added to minimize the effects of heat release because of the exothermic hydration process. The mixture was stirred to obtain a gel, similar to mortar. The gel was extruded through a 1.0 mm sieve to obtain uniform pellet diameters. The resulting pellets were then air-dried for 24 h, and the final pellets obtained had diameters of ~0.8 mm. More details on the limestone and pellets, their composition, and the pellet preparation method are presented elsewhere.[32]

A Mettler Toledo TGA/SDTA851^e/LF/1100 °C thermogravimetric analyzer (TGA) was used for the calcination/carbonation cycles. The sample was placed in a ceramic pan (5 mm inner diameter). The temperature and gas used were controlled by STARe software. Two types of calcination/carbonation cycles were carried out: (1) The temperature program started with heating to 950 °C under an atmosphere of 100% CO_2. When the temperature reached 950 °C (sample was calcined), the CO_2 gas stream was replaced with a gas mixture of 20% CO_2 and N_2 balance and cooling to 800 °C was started. After the temperature reached 800 °C, the gas flow was maintained for 30 min (carbonation). After this step, the gas mixture was replaced with CO_2, heating to 950 °C simultaneously commenced, and these cycles were repeated. (2) The temperature program started with heating to 800 °C under an atmosphere of 100% N_2. After that, the temperature was constant (800 °C) to the end of experiment. At 15 min after the temperature had reached 800 °C (the sample was calcined), the CO_2 gas stream was replaced with a gas mixture of 20% CO_2 and N_2 balance for 30 min (carbonation).

The heating/cooling rate during runs was 50 °C/min. The gas flow rates were controlled with flow meters at 40 cm^3/min. The calcination/carbonation cycles were performed typically 1, 3, 10, 30, and 100 times.

The sample was removed from the TGA after cycles and examined by a scanning electron microscope (SEM). A Hitachi S3400 microscope with 20 kV of accelerating voltage was used. The samples were crushed to expose their inner parts to the electron beam and coated with a 3 nm thick layer of gold−palladium.

Results and Discussion

Calcination/carbonation cycles in this study were performed under different conditions, with natural limestone and synthetic sorbent. Series with 1, 3, 10, 30, and 100 cycles were performed, and samples after the last carbonation stage were examined by a SEM. Additionally, some of the samples were calcined after the last carbonation to observe them in a calcined form.

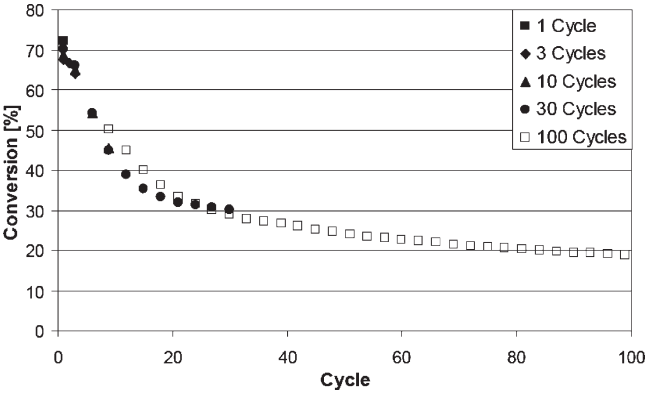

Figure 1. Conversions during calcination/carbonation cycles of KR limestone, with a particle size of 600−750 μm. Conditions: calcination in 100% N_2 at 800 °C for 15 min and carbonation in 20% CO_2 (N_2 balance) at 800 °C for 30 min.

The conversions during the series of calcination/carbonation cycles with natural limestone (in the case of calcination in nitrogen) are presented in Figure 1. It can be seen that there is relatively high repeatability of the results for the different series of cycles and, as is typical for such cycles, the sorbent rapidly loses its activity. It is assumed that the main cause is sintering and the loss of both the sorbent surface area and small pore volume.[21−24] This results in a rapid transition from the fast reaction stage to the slow reaction stage controlled by diffusion through the formed product layer. The results presented in Figure 1 show that the activity of this limestone falls from >70% in the first cycle to <20% after 100 cycles.

In addition, evidence in the literature[21] exists that the sintering may result in "bottlenecks" close to the sorbent particle surface. The detailed SEM examination of both carbonated and calcined residues after cycles in this study also showed this tendency. The characteristic SEM images are presented in Figure 2 for carbonated samples after the 1st and 100th cycle and show that a thin carbonate shell (~1 μm) can be formed even after the first cycle (a). A view of the outer particle surface (b) shows that there are areas with different levels of sintering at irregular locations. The significantly different morphology can also be seen in the particle interior with defined grain structure (c). The space between the grains, i.e., the porosity, is very low because of the high conversion, >70%.

A similar morphology with more pronounced sintering at the particle surface than that in the interior can be seen after 3, 10, 30, and 100 cycles, and SEM images for 100 cycles are presented in panels d−f of Figure 2. It might be expected that, given that the sorbent is more sintered because it was subjected to the longer series of cycles, the difference between the outer shell and interior texture would be more pronounced. However, this is not seen here because of the very low conversion (<20%). Namely, despite the larger grains seen in Figure 2e when compared to those seen in Figure 2b, they are not fully coalesced. Moreover, pore cracks can be seen at the sorbent particle surface (f). In general, it can be assumed that in the event of prolonged carbonation time and/or with higher conversion, a carbonate shell would be formed (see below).

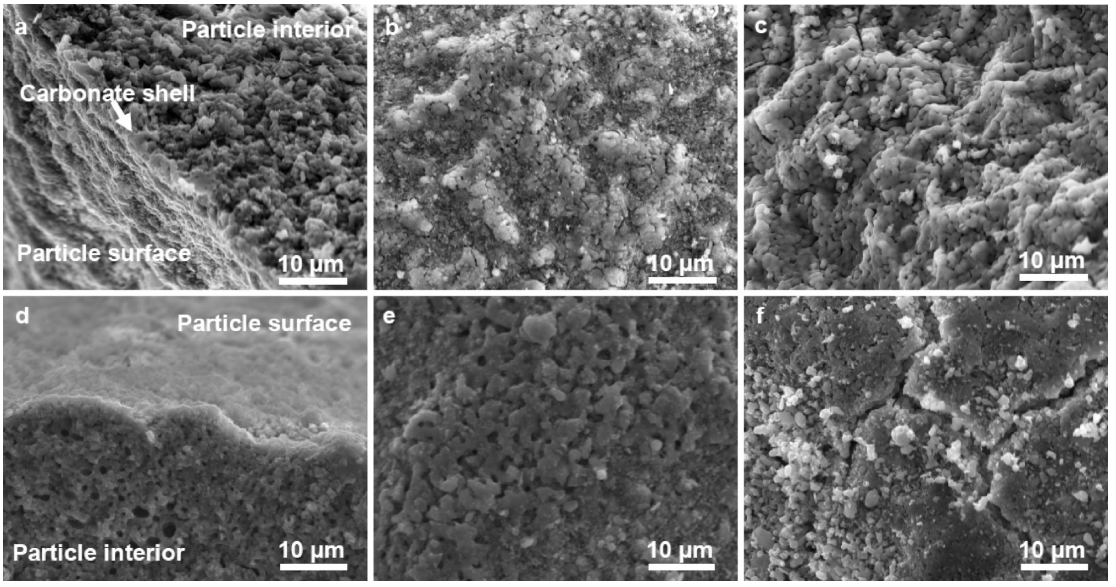

Figure 2. SEM images of KR samples after calcination/carbonation cycles presented in Figure 1: (first row) (a) broken particle, (b) particle surface, and (c) particle interior after 1 cycle and (second row) (d) broken particle and (e and f) particle surface after 100 cycles.

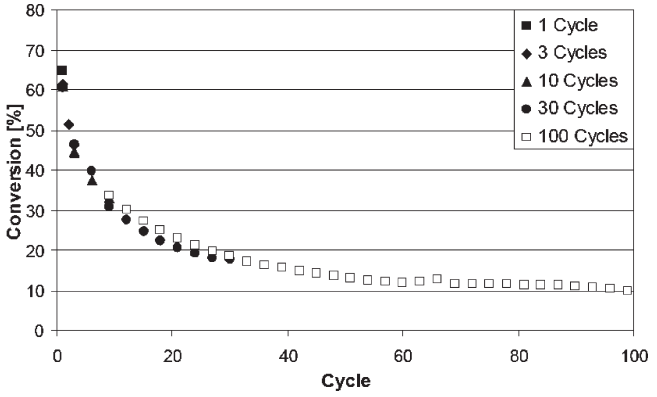

Figure 3. Conversions during calcination/carbonation cycles of KR limestone, with a particle size of 600−750 μm. Conditions: calcination in 100% CO_2 at 950 °C and carbonation in 20% CO_2 (N_2 balance) at 800 °C for 30 min.

Calcination at higher temperature (950 °C) in a concentrated stream of CO_2 results in faster sintering and the loss of activity during CO_2-capture cycles, and an example of this is presented in Figure 3. This is a consequence of enhanced sintering at high temperature and high CO_2 concentration. The final result is very low conversion, 10%, after 100 cycles, which is about half that obtained under milder conditions (Figure 1). The SEM examination of samples at the end of this series of calcination/carbonation cycles also shows more pronounced sintering at the sorbent particle surface. The most characteristic SEM images are presented in Figure 4. The carbonate shell is locally formed even after the first carbonation (a). The interior morphology again differs from that at the particle surface (b). After 100 cycles (c), the $CaO/CaCO_3$ grains in the interior of the particle are noticeably larger and more spherical than those after the first cycle (b). The surface carbonate shell is formed but often broken, forming large cracks with an order of magnitude of micrometers.

The SEM work performed in this study showed that a carbonate shell is always formed and is typically more intensive after longer series of cycles, but quantifying this fully was not possible by the SEM analyses performed here. For example, it was not possible to measure the thickness and porosity of this shell after different series of calcination/carbonation cycles. These samples after different numbers of cycles had different levels of carbonation conversions. Moreover, the samples display distinct areas with uneven intensity of sintering; i.e., their surface is heterogeneous (see for example panels b and e of Figure 2).

The increased sintering at the particle surface results in a higher probability of formation of nonporous areas that prevent diffusion of CO_2 toward the interior of the particle. It is reasonable that, with higher conversions, these nonporous areas become larger and more abundant and finally coalesce, forming a nonporous shell, which would then effectively prevent any further carbonation. Such a phenomenon would probably not be seen in practice because CaO-based CO_2-looping cycles are designed so that only the fast reaction stage is used for CO_2 capture, and this takes place over at most 5−10 min. However, here, a longer carbonation time is applied to reach higher conversions and help quantify the intensity of surface sintering.

Conversions after prolonged carbonation of limestone samples (after different numbers of cycles) are presented in Figure 5. It can be seen that the first carbonation after calcination in N_2 reaches a value of ~80%, which is ~10% higher than that when the sample was calcined in CO_2. The lower "final" conversion for the sample calcined in CO_2 is in agreement with previous studies on the influence of calcination conditions on CaO-carrying activity.[35] However, the most interesting result here is the decrease in final conversions after 5 h carbonation as the number of cycles that the samples experienced before prolonged carbonation increases. Moreover, the carbonation/time profiles differ in their shape. To explain these results, further factors are considered.

The first limit appears to be due to the change of the sorbent particle morphology during cycles, which reduces the available surface area for the reaction. This limits the conversion after the fast, kinetically-controlled reaction step because of product layer formation.[24] However, the product layer formation in the interior of the particle cannot explain the limited conversion after prolonged carbonation. Namely, that explanation would imply the hypothesis of two critical product

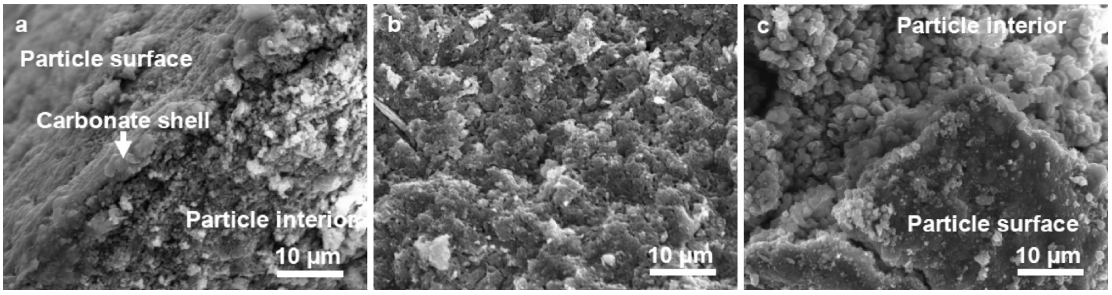

Figure 4. SEM images of KR samples after calcination/carbonation cycles presented in Figure 3: (a) broken particle and (b) particle interior after 1 cycle and (c) broken particle after 100 cycles.

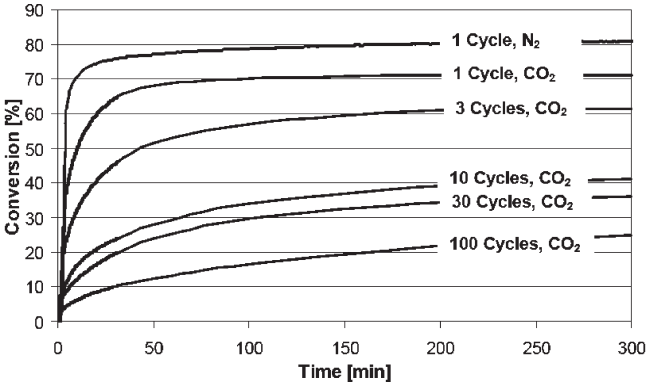

Figure 5. Conversion profiles in prolonged (5 h) last carbonation of KR limestone, with a particle size of 600−750 μm, subjected to different series of cycles. Conditions during cycles are the same as those for Figure 3 (except for 1 cycle, N_2, Figure 1).

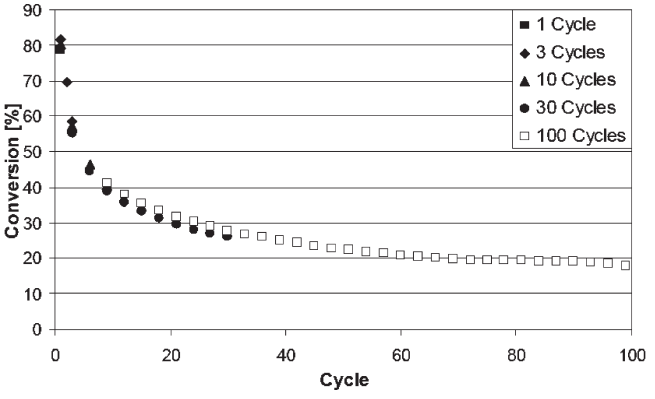

Figure 6. Conversions during calcination/carbonation cycles of KR-CA-14 pellets, with a particle size of ∼0.8 mm. Conditions: calcination in 100% CO_2 at 950 °C and carbonation in 20% CO_2 (N_2 balance) at 800 °C for 30 min.

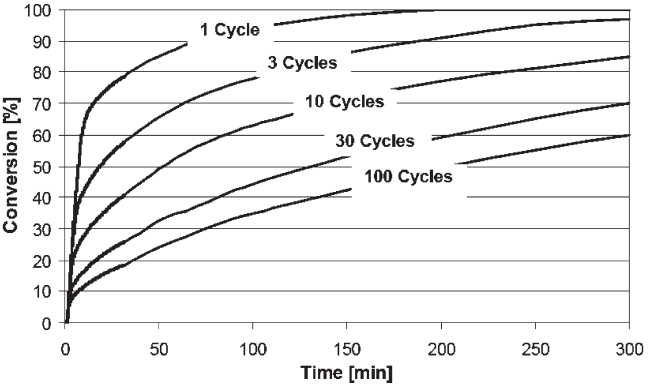

Figure 7. Conversion profiles in prolonged (5 h) last carbonation of KR-CA-14 pellets, with a particle size of ∼0.8 mm, subjected to different series of cycles. Conditions during cycles are the same as those for Figure 6.

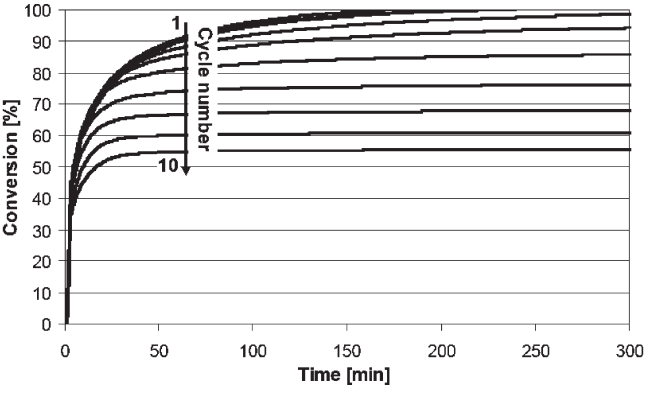

Figure 8. Conversion/time profiles during calcination/carbonation cycles of KR-CA-14 pellets, with a particle size of ∼0.8 mm. Conditions: calcination in 100% CO_2 at 950 °C and carbonation in 20% CO_2 (N_2 balance) at 800 °C for 5 h.

layer thicknesses, the first one after the fast reaction step (already postulated)[24] and another one during the diffusion-controlled reaction stage. The postulation of the second critical product layer thickness does not appear to make sense. Namely, when a critical product layer thickness is reached once, it can be expected that the reaction after that is controlled by diffusion in that layer and should become slower with increasing product layer thickness but full conversion should be reached without further limits related to that product layer.

The additional limit appears because, during cycles, the sorbent particles shrink, as can be demonstrated by measuring pellet dimensions before and after cycling,[38] where the loss of the particle volume was about 15−20%. A similar phenomenon has also been demonstrated by mercury porosimetry[39] and powder and helium displacement pycnometry results[35] for natural limestones. This phenomenon reduces pore volume in the sorbent, which limits the available space for bulky product ($CaCO_3$) storage during the reaction.

(38) Manovic, V.; Anthony, E. J. The long-term behavior of CaO-based pellets supported by calcium aluminate cements in long series of CO_2 capture cycles. *Ind. Eng. Chem. Res.* **2009**, *48*, 8906–8912.

(39) Manovic, V.; Anthony, E. J.; Loncarevic, D. CO_2 looping cycles with CaO-based sorbent pretreated in CO_2 at high temperature. *Chem. Eng. Sci.* **2009**, *64*, 3236–3245.

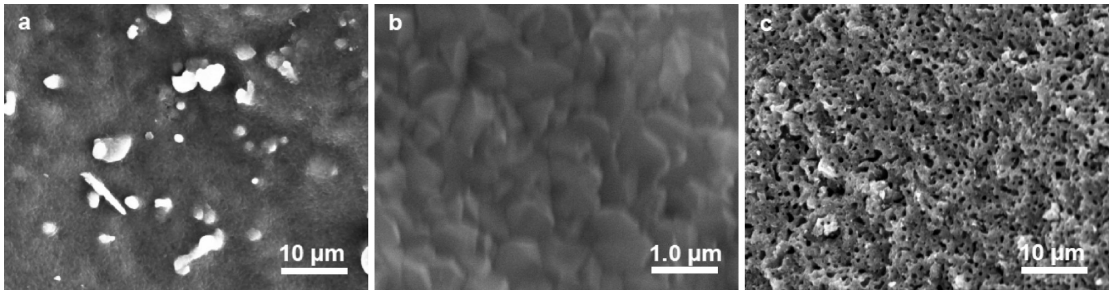

Figure 9. SEM images of KR-CA-14 pellets after 10 calcination/carbonation cycles presented in Figure 8: (a and b) particle surface and (c) particle interior.

Another effect considered in this study is enhanced sintering at the surface of the sorbent particle, and this can provide an explanation for the limit in conversion after prolonged carbonation. With increasing numbers of cycles, sintering at the surface becomes more pronounced and prevents diffusion of CO_2 toward the particle interior. To provide additional support for this hypothesis, experiments were performed with a synthetic CaO/Al_2O_3-based sorbent, which is more porous, and limits because of the loss of the surface area and small pore volume are consequently less pronounced. Conversions during different series of cycles with KR-CA-14 pellets are presented in Figure 6. As can be seen, this sorbent has higher conversions during the various cycles than shown by the natural limestone (Figure 3). Moreover, it has already been previously reported[36] that better performance of the synthetic sorbent is more pronounced when the carbonation time is longer.

Prolonged carbonation of samples after different numbers of cycles was carried out, and conversion/time profiles are presented in Figure 7. These profiles show higher conversions than those seen for natural sorbent (Figure 5). Moreover, the synthetic sorbent is able to reach near-quantitative conversion, which is the case for the first carbonation cycle after 3 h. This is a significant difference from natural limestone, where the maximum conversion reached is ~80%. The long-term conversion curves of other samples obtained after 3−100 cycles display higher conversion versus time gradients than those seen for natural limestone in Figure 5. This means that additional limits, other than those related to the product layer diffusion, are much less pronounced in the synthetic sorbent.

However, to demonstrate that shell formation also occurs at the surface of synthetic pellets, an additional 10-cycle experiment was performed with 5-h carbonation periods. The conversion profiles obtained are presented in Figure 8. The first three conversion profiles overlap, and quantitative conversions were achieved after ~3 h. However, with increasing cycle number, the limit in conversion becomes more pronounced and appears earlier, and by the 10th cycle, the maximum conversion of ~55% was reached after 1 h. Further exposure of the sample to a CO_2 atmosphere for 4 h resulted in a negligible conversion increase (~0.1%). These results indicate that a carbonate shell was also formed at the pellet surface.

The formation of a nonporous carbonate shell can be clearly seen in panels a and b of Figure 9. It can be seen at higher magnification (b) that $CaCO_3$ grains/crystals of an order of magnitude of hundreds of nanometers form a totally nonporous surface. This prevents diffusion of CO_2 toward the particle interior, where unreacted CaO and porous CaO exist (c). Despite the very porous structure of the pellet particle (c), carbonation is blocked by the outer carbonate shell, and this suggests that the carbonation reaction is relatively fast, thus allowing the formation of a shell, despite the presence of ample porosity in the interior of the particle.

It can be supposed that during cycles the sorbent particles shrink, as already demonstrated.[35,38,39] Furthermore, it can be expected that the loss of sorbent volume occurs more strongly at the particle surface than in its interior; which is an effect similar to surface tension, as seen in liquids.[40] Namely, the grains inside sorbent particles are totally surrounded by other grains, but at the particle surface, this is not the case. Thus, the interior structure is more resistant and less liable to see a loss of volume, and this enables it to retain a network of pores and solid skeleton (Figure 9c). On the other hand, the grains at the surface are more mobile. Hence, during calcination/carbonation cycles, they migrate closer and, finally, because of their swelling, resulting from the formation of the more voluminous $CaCO_3$ product [$VM(CaCO_3):VM(CaO) = 36.9\ cm^3/mol:16.9\ cm^3/mol$], form a nonporous shell (panels a and b of Figure 9).

These results are obtained under extreme conditions, i.e., very long carbonation periods (5 h), and they clearly show the formation of a carbonate shell/partially carbonated core pattern. Moreover, the results obtained in this study for a 30-min carbonation time also show the formation of more sintered and less porous areas at the sorbent surface than that seen in the particle interior. These findings can lead to further directions in the preparation of synthetic sorbents, which involves coating of sorbent particles by a material more resistant to sintering. The role of this outer shell should be to reduce sintering at the particle surface and to increase particle strength.

Conclusions

Enhanced sintering and the formation of a carbonate shell on sorbent particles is investigated in this paper. It is shown that the sorbent surface is more liable to sintering during series of calcination/carbonation cycles. The thickness of this sintered area/shell is an order of magnitude of micrometers. The SEM analyses of partially carbonated sorbent particles show that it is a nonporous material that locally or totally prevents diffusion of CO_2 toward the partially reacted sorbent core. This reduces the rate of conversion and/or finally prevents further reaction. The fast reaction stage is not affected by this effect because a carbonate shell is not present at the beginning of carbonation in a particular calcination/carbonation cycle. Prolonged carbonation showed that, in addition to the conversion maximum after the fast, kinetically-controlled reaction step (attributed to filling small pores/formation of a critical product layer), there is another limit to "maximum"

(40) Adamson, A. W. *Physical Chemistry of Surfaces*, 5th ed.; John Wiley and Sons, Ltd.: New York, 1990.

conversion that can also be attributed to closure of pores close to the sorbent particle surface (formation of a carbonate shell). The proposed deactivation mechanism because of the formation of a carbonate shell at the sorbent particle surface (several micrometers thick) does not negate the deactivation mechanism because of the formation of the product layer at the sorbent surface area (∼50 nm). It can be expected that these two deactivation limits overlap after an initial kinetically controlled reaction stage. The results presented in this paper can result in further directions in the preparation of synthetic sorbents, which involves coating of sorbent particles by a more sintering-resistant material.